## SENSITIVITY OF LES SIMULATIONS TO RESOLUTION, SUBGRID MODELS AND BOUNDARY CONDITIONS

*Vladimír Fuka[1], Jelena Radović[1] and Štěpán Nosek[2]*

[1]Department of Atmospheric Physics, Faculty of Mathematics and Physics, Charles University, Prague, Czech Republic
[2]Institute of Thermomechanics, Czech University of Sciences, Prague, Czech Republic

**Abstract**: Sensitivity of large eddy simulations of flow and passive scalar dispersion in idealized urban canopy. The main variable followed are the boundary conditions and the domain size. The effect on convergence to homogeneous time-averaged solution and temporal spectra is investigated.

*Key words: large eddy simulation, sensitivity, convergence, boundary conditions*

### INTRODUCTION

It is common to investigate the flow in certain types of urban canopy using large eddy simulation (LES) in idealized conditions. Often, periodic boundary conditions are used to simulate a fully developed flow over an "infinite" canopy (e.g., Castro et al., 2017). Another option are turbulent inflow boundary conditions (Sessa et al., 2018). The scalar boundary conditions are typically non-periodic in either case. This work examines the effect of the periodic boundary conditions on the simulated flow and the resulting scalar dispersion in an idealized urban canopy.

The selected configuration of building of canopy with closed courtyards follows (Kluková et al., 2020) and was previously measured in wind-tunnel experiments. Only the case with uniform roof height and pitched roofs was considered for simplicity. This particular case showed the biggest discrepancy in the mean flow from the wind tunnel experiments in earlier simulations and deserves further investigation

### NUMERICAL CODE, SIMULATION SETUP

#### Numerical model

The ELMM in-house code (Fuka, 2015) was used. ELMM solves the incompressible Navier-Stokes equations on a uniform Cartesian grid with the immersed boundary method used for solid bodies. The equations are discretized using the finite volume method with second order central spatial differences. For temporal discretization, a third-order Runge-Kutta method and the projection method are used. The mixed-time-scale (MTS) model by Inagaki et al. (2005) is used for subgrid stresses. Synthetic turbulent inflow boundary conditions are generated using the method of Xie and Castro (2008).

#### Setup of the simulations

The default domain originates from (Kluková et al., 2020) and comprises 4 x 4 blocks with courtyards. Each block has dimensions 2.4 H x 4.8 H (streamwise x spanwise), where H is the building height. The total dimensions of the domain are 12.8 H x 22.4 H. The default domain is visualized in Figure 1 a). The grid resolution was 18.75 cells / H in the streamwise directions and 20 cells / H in the vertical direction.
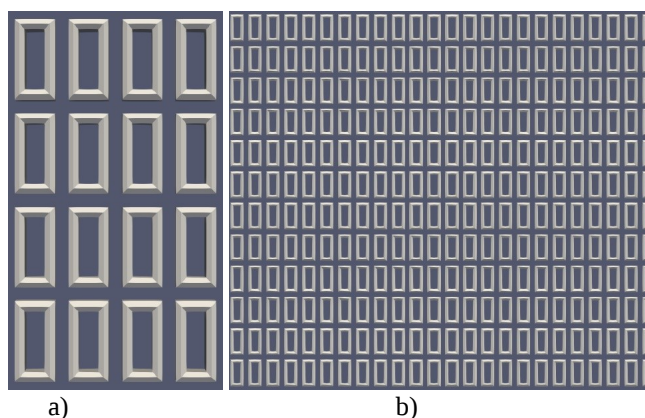
Figure 1. The default (a) and the largest (b) computational domain and the layout of the blocks of buildings around the courtyards.

Larger domains were tested. The extended domain was extended 2x in the streamwise direction, extended domain 2 was extended 4x in the streamwise direction, the very large domain 6x in the streamwise direction and 3x in the spanwise direction. The largest domain is shown in Figure 1 b). For this largest domain the grid resolution had to be reduced.

A different domain was used for simulations with turbulent inflow boundary conditions. It corresponds to the default domain extended 2x in the streamwise direction with short empty sections appended at the inflow and the outflow.

**RESULTS AND DISCUSSION**
The first comparison considers instantaneous and time-averaged velocity fields in domains of varying size. The periodic boundary conditions prohibit structures longer than the streamwise domain size and wider than the spanwise domain width. Moreover, a certain structure, e.g., a region of higher or slower wind speed, can cycle in a certain spanwise location many times and hence generate a negative or positive bias of wind speed. For turbulent inflow boundary conditions, the situation is different because the structures are generated with the same mean value across the span and the timescale is dictated by the generating algorithm. However, close to the inflow plane the turbulent fields are affected by the synthetic generation and need some travel time to adjust.

Instantaneous structures of the streamwise velocity component in the four configurations at z = 1.2 H are depicted in Figure 2. One can notice that even for the largest domain the structures are very long.
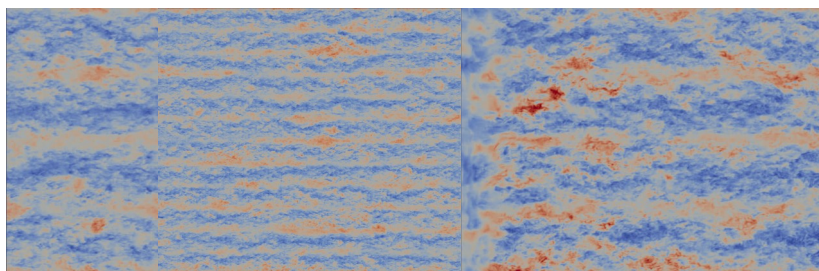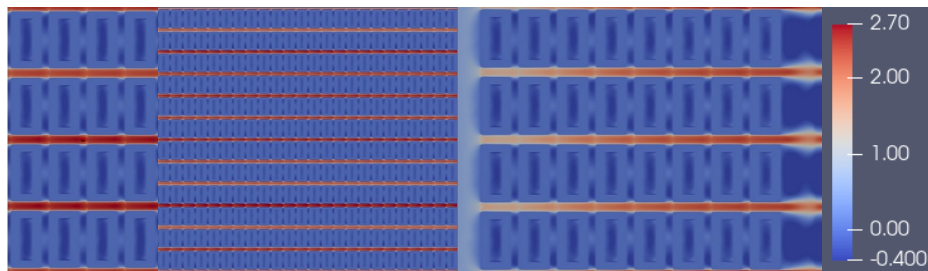


Figure 2. Instantaneous snapshots of spanwise wind velocity at height z = 1.2H for a) the default domain with periodic boundary conditions, b) the largest domain with periodic boundary conditions, c) the domain with inflow boundary conditions.

The time-averaged streamwise velocity field at the same height are shown in Figure 3 and the effect on time-averaged streamwise velocity inside the canopy (z = 0.4 H) are shown in Figure 4. The averaging time was equal in all cases to 320 H/u∗. One can clearly identify streets that are faster and streets that are slower. That also leads to asymmetric dispersion patterns (not shown here) from scalar sources located

between the streets with different wind speed. For inflow boundary conditions the wind speed is equal across the span but it changes in the streamwise direction as the flow develops.
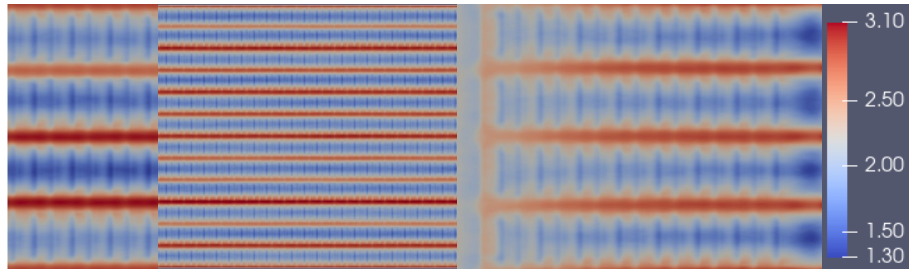


**Figure 3.** Time-averaged fields of spanwise wind velocity at height z = 1.2 H for a) the default domain with periodic boundary conditions, b) the largest domain with periodic boundary conditions, c) the domain with inflow boundary conditions.



**Figure 4.** Time-averaged fields of spanwise wind velocity at height z = 0.4 H for a) the default domain with periodic boundary conditions, b) the largest domain with periodic boundary conditions, c) the domain with inflow boundary conditions.

We also investigated the temporal spectra of the streamwise velocity component at a fixed point above the canopy, namely at point above the central intersection at the height of 2 H in Figure 5. The results are compared to wind-tunnel measurements at the height of 1.6 H. For the largest domain the variance is lower due to lower grid resolution because the results are scaled by the variance of the resolved velocity component. One can see that the peak dictated by the domain size moves to lower frequencies but remains present even for the largest domain, which is much longer than the size of the area modelled in the wind tunnel experiment. Figure 6 compares the streamwise velocity spectra for two settings of the integral timescale for the synthetic turbulence generator. The spectra do not show such distinct peak but clearly contain much fewer low-frequency structures compared to the wind tunnel.
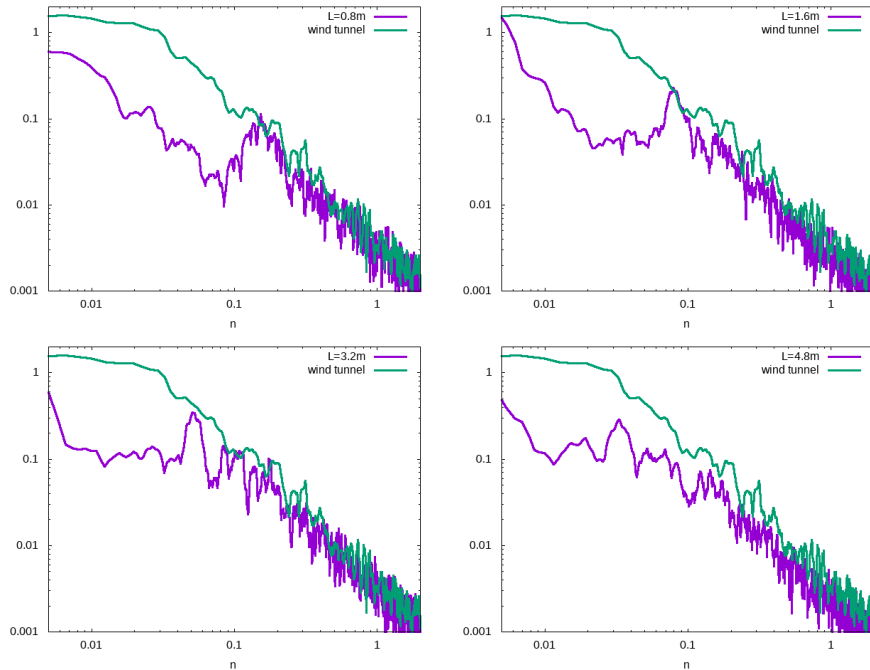
**Figure 5.** Dimensionless spectra of the streamwise velocity component at z = 2 H compared to wind-tunnel measurements at z = 1.6 H for different domain sizes with peridic boundary conditions. Domain length indicated in meters, H = 6.25 cm.
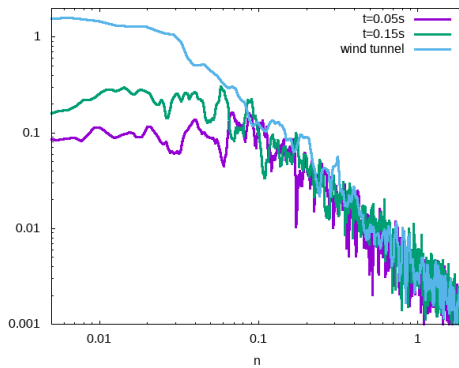


**Figure 6.** Dimensionless spectra of the streamwise velocity component at z = 2 H compared to wind-tunnel measurements at z = 1.6 H for two different integral time scale settings of the synthetic turbulence generator.

## CONCLUSION

A subset of sensitivity tests performed for the flow in an idealized periodic urban canopy with uniform building heights is presented. The results show the effect of periodic and turbulent inflow boundary conditions on instantaneous and time-averaged flow fields. The periodic boundary conditions affect the convergence to homogeneous averaged solution by promoting structures of higher and lower wind speed to remain locked in a certain spanwise location and being recycled over the same location several times. The turbulent inflow conditions do not exhibit this problem but the flow develops in the streamwise direction and the synthetic turbulent flow needs a certain time to develop to a more natural flow. The velocity spectra are also affected and show the large importance of the structures corresponding to the streamwise domain length. Increasing the domain size did not result in improved convergence to a solution homogeneous across the span.

Other tests were performed but cannot be shown in this short contribution. They include test of grid convergence in a small domain comprising a single building block. The contribution of subgrid modelling was also tested in different grid resolution by using different subgrid models and also by performing DNS in lower Reynolds number by increasing the value of air viscosity and scalar diffusivity. These tests also included scalar dispersion and will be a topic of future publications.

**REFERENCES**
Castro, I.P., Z.-T. Xie, V. Fuka, A.G. Robins, M. Carpentieri, P. Hayden, D. Hertwig and O. Coceal, 2017: Measurements and Computations of Flow in an Urban Street System, *Boundary-Layer Meteorol.*, **162**, 207-230.
Fuka, V, 2015: PoisFFT – A free parallel fast Poisson solver, *Applied Mathematics and Computation*, **267**, 356-364.
Inagaki, M., T. Kondoh and Y. Nagano, 2005: A Mixed-Time-Scale SGS Model With Fixed Model-Parameters for Practical LES, *J. of Fluids Eng.*, **127**.
Kluková, Z., Š. Nosek, V. Fuka, Z. Jaňour, H. Chaloupecká and J. Ďoubalová, 2021: The combining effect of the roof shape, roof-height non-uniformity and source position on the pollutant transport between a street canyon and 3D urban array, *J. of Wind Eng. & Industrial Aerodyn.*, **208**.
Sessa, V., Z.-T. Xie and S. Herring, 2018: Turbulence and dispersion below and above the interface of the internal and the external boundary layers, *J. of Wind Eng. & Industrial Aerodyn.*, **182**, 189-201.
Xie Z.-T. and I.P. Castro, 2008: Efficient Generation of Inflow Conditions for Large Eddy Simulation of Street-Scale Flows, *Flow Turbulence Combust.*, **81**, 449–470.